ACS APPLIED MATERIALS & INTERFACES

Research Article

www.acsami.org

Soft Contact Transplanted Nanocrystal Quantum Dots for Light-Emitting Diodes: Effect of Surface Energy on Device Performance

Hyunduck Cho,[†,¶] Jeonghun Kwak,[*,∥,¶] Jaehoon Lim,[⊥] Myeongjin Park,[†] Donggu Lee,[†] Wan Ki Bae,[#] Youn Sang Kim,[‡] Kookheon Char,[§] Seonghoon Lee,[Δ] and Changhee Lee[*,†]

[†]School of Electrical and Computer Engineering, Inter-university Semiconductor Research Center (ISRC), [‡]Program in Nano Science and Technology, Graduate School of Convergence Science and Technology, and [§]School of Chemical and Biological Engineering, Seoul National University, Seoul 151-744, Korea

[∥]Department of Electronic Engineering, Dong-A University, Busan 604-714, Korea

[⊥]Center for Advanced Solar Photophysics, Los Alamos National Laboratory, Los Alamos, New Mexico 87545, United States

[#]Photo-Electronic Hybrids Research Center, Korea Institute of Science and Technology (KIST), Seoul 136-791, Korea

[Δ]Department of Chemistry, Seoul National University, Seoul 151-747, Korea

Supporting Information

ABSTRACT: To realize the full-color displays using colloidal nanocrystal quantum dot (QD)-based light emitting diodes (QLEDs), the emissive QD layer should be patterned to red (R), green (G), and blue (B) subpixels on a micrometer scale by the solution process. Here, we introduced a soft contact QD-transplanting technique onto the vacuum-deposited small molecules without pressure to pattern the QD layer without any damage to the prior organic layers. We examined the patternability of QDs by studying the surface properties of various organic layers systematically. As a result, we found that the vacuum-deposited 4,4′,4″-tri(*N*-carbazolyl)triphenylamine (TCTA) layer is suitable for QD-transplanting. A uniform and homogeneous QD patterns down to 2 μm could be formed for all the RGB QDs (CdSe/CdS/ZnS, CdSe@ZnS, and $Cd_{1-x}Zn_xS$@ZnS, respectively) with this method. Finally, we demonstrated the R, G, and B QLEDs by transplanting each QD onto the soft TCTA layer, exhibiting higher brightness (2497, 14 102, and 265 cd m^{-2}, respectively) and efficiency (1.83, 8.07, and 0.19 cd A^{-1}, respectively) than those of the previous QLEDs fabricated by other patterning methods. Because this pressure-free technique is essential for patterning and stacking the QDs onto the soft organic layer, we believe that both fundamental study and the engineering approach presented here are meaningful for the realization of the colloidal QD-based full-color displays and other optoelectronic devices.

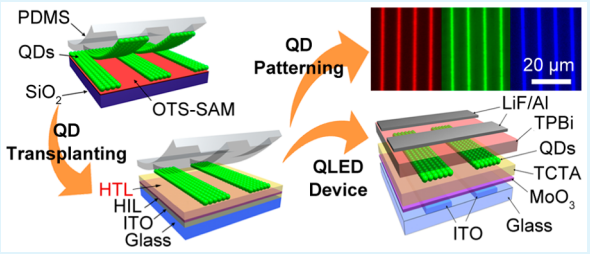

KEYWORDS: *quantum dot light-emitting diodes, quantum dots, transfer printing, surface energy, pressure free, transplanting*

INTRODUCTION

The interest in colloidal nanocrystal quantum dot (QD)-based light emitting diodes (QLEDs) has been growing due to their excellent properties, such as narrow emission bandwidths by the quantum confinement effect, emission wavelength tunability, and solution processability.[1−5] Several years of multifaceted efforts on material synthesis,[6−10] electrophysical analysis,[11−14] and device design[15−17] also have improved the device performance of the QLEDs comparable to that of organic light-emitting diodes (OLEDs). In particular, the recent demonstration of a QLED-based full-color display made the QLEDs be one of the most promising candidates for display devices.[18]

To produce the full-color QLED display devices, patterning the different colored QDs (e.g., red (R), green (G), and blue (B) QDs) on a micrometer scale is inevitably required to separate RGB pixels. However, it is not easy to form the fine patterns of RGB QDs in one emissive layer because the sequential deposition/patterning processes of each QD solution can spoil the prior QD patterns. To make the QD layer patterned, various QD "printing" methods, such as inkjet printing,[19−21] contact/transfer printing,[22−29] and 3D printing,[30] have been reported. Among these printing techniques, the contact/transfer printing method using poly(dimethylsiloxane) (PDMS) as a stamp has been introduced by the advantage of making conformal contact with a substrate surface due to its low adhesion property.[31] In addition, the morphology of the QD patterns fabricated in this technique is generally much smoother than those obtained by other printing methods. However, PDMS, the elastomeric stamp easily contorts and swells up by most of organic solvents which are used for dispersing QDs. Moreover, during the printing process, the underlying functional organic layers in QLED devices can be damaged. To overcome this issue, researchers adopted a rigid

Received: February 25, 2015
Accepted: May 5, 2015
Published: May 5, 2015

DOI: 10.1021/acsami.5b01738
ACS Appl. Mater. Interfaces 2015, 7, 10828−10833

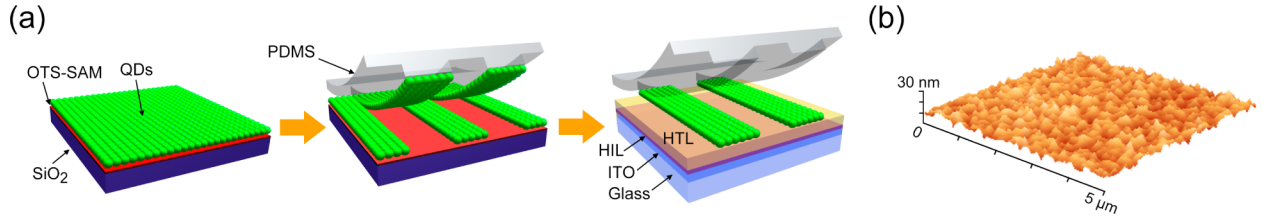

Figure 1. (a) Schematic diagrams of the QD-transplanting process and (b) the surface image of the transplanted QD film measured with an AFM.

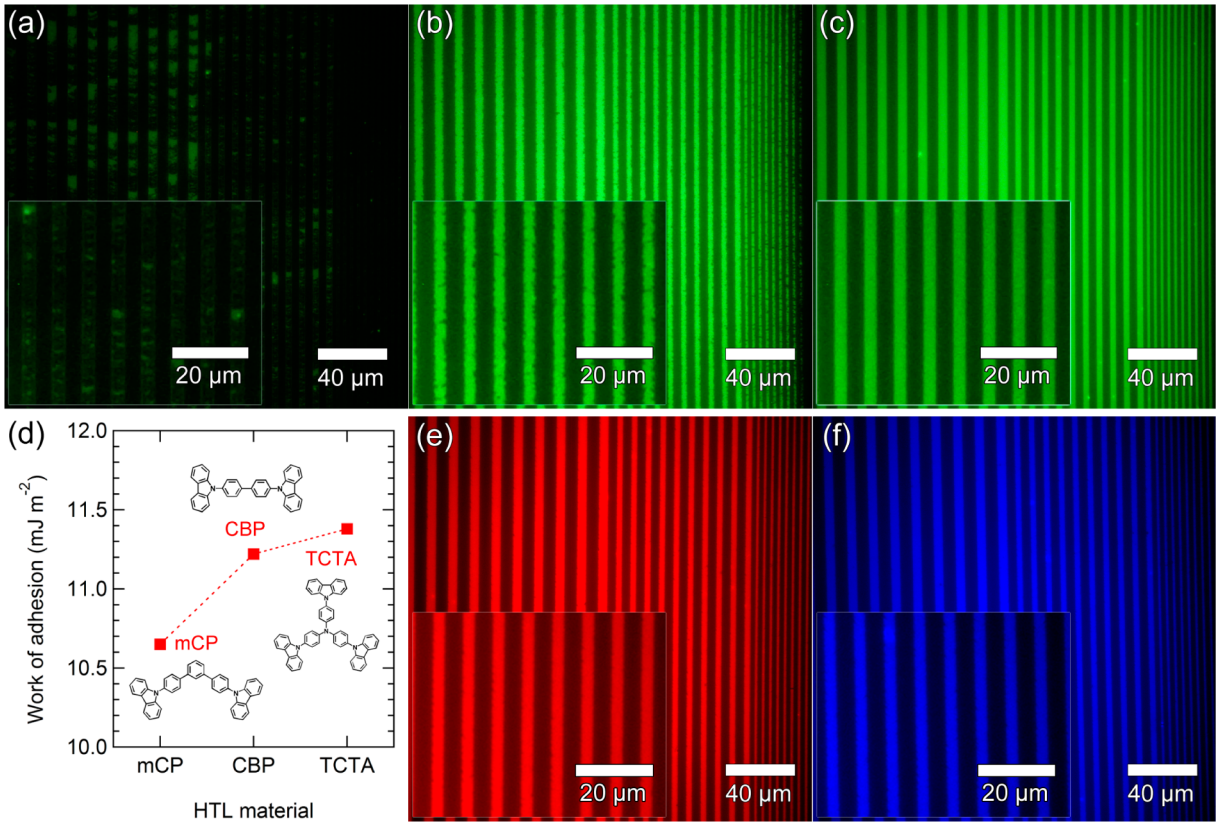

Figure 2. FOM images of the stripe-patterned green QDs on (a) mCP, (b) CBP, and (c) TCTA films using the transplanting method. Insets in each figure are the magnified FOM images of the 4 μm stripes. (d) Plots of the work of adhesion values between each HTM and the green QDs on the PDMS, and the chemical structures of the HTMs. The FOM images of the transplanted (e) red and (f) blue QDs on the TCTA film.

protection layer (e.g., parylene-C or SU-8) on the PDMS,[25] and used cross-linkable materials in the hole transport layer (HTL) and/or the QD layer.[18,22] A few QLEDs and QLED displays have been demonstrated recently using these techniques, but those cross-linkable materials require an additional annealing process to make them hard with a high temperature. Furthermore, there are just a few choices of the cross-linkable hole transporting materials (HTMs) possessing low values of the highest-occupied-molecular-orbital (HOMO) energy level for easy hole injection into the QDs. Another reason for using the rigid polymeric HTL was that a high pressure (196 kPa) was applied to the organic HTL in the QD-transferring procedure in previous work.[18,22] Although we have plenty of options for small molecule HTMs having a deep HOMO level, it is impossible for the vacuum-evaporated soft organic layers to endure such a high pressure. Moreover, due to the weak adhesion between the organic HTMs and the prior layer (e.g., electrodes or hole injection layer), the organic layer can be detached during the transfer process unless the surface properties of the stamps are controlled precisely. Thus, to transfer and pattern the RGB QDs on the vacuum-deposited soft organic layer, reducing the pressure to the receiving substrate is required. Also, it is important to control the surface energy and adhesion between the organic HTL, the QD film, and the surface of the PDMS stamp.

Here we show a "QD-transplanting" technique, which is a method for transferring a patterned QD layer onto a vacuum-deposited small molecule HTL with little pressure, based on a systematic investigation of the surface properties (i.e., the surface energy of various organic HTMs and the work of adhesion) between the HTMs on a glass substrate and the QDs on the PDMS stamp. Using this method, we successfully demonstrated the full-color QLEDs consisting of the transplanted R, G, and B QDs (CdSe/CdS/ZnS, CdSe@ZnS, and $Cd_{1-x}Zn_xS$@ZnS, respectively) on the vacuum-deposited 4,4′,4″-tri(*N*-carbazolyl)triphenylamine (TCTA) layer which possesses a deep HOMO energy level.

DOI: 10.1021/acsami.5b01738
ACS Appl. Mater. Interfaces 2015, 7, 10828−10833

RESULTS AND DISCUSSION

The transplanting technique is a simple, dry, and nondestructive process to the underlying organic layers. The specific process illustrated in Figure 1a is as follows: first, QDs were spun onto a SiO_2 substrate treated with octadecyltrichlorosilane (OTS) self-assembled monolayer (SAM) to help the QD film detach easily from the substrate. After that, the UV-ozone-treated PDMS stamp was placed on the QDs/OTS/SiO_2 substrate for 10 s with no additional pressure, and then the stamp was peeled off. Finally, the QD-inked PDMS stamp was attached to the receiving substrate without pressure for 10 s and peeled off. The receiving substrate was prepared by vacuum evaporation, consisting of the MoO_3 as a hole injection layer (HIL) and TCTA as the HTL, on top of the indium−tin oxide (ITO) glass substrate. A smooth and homogeneous QD film was successfully formed on the vacuum-deposited TCTA layer by this technique, as shown in the atomic force microscopy (AFM) image in Figure 1b. The root-mean-square roughness of the surface was 3.52 nm. To clarify the comparative advantage of the transplanting method to the pressure-assisted contact printing, we applied pressure during the QD printing onto the TCTA layer. We found that the transferred QD layers cracked as shown in Figure S1 in Supporting Information. Because the pressure-assisted transfer of the QD film onto the polymer HTL was already demonstrated without any defects in the QD film, the cracks are possibly attributed to the break of the underlying TCTA layer. In other words, our soft contract transplanting method is a superb technique for printing QD thin films onto the vacuum-deposited small molecule layers.

As mentioned previously, the HOMO energy level of the HTL should be low for efficient hole injection into QDs. For this purpose, we chose three carbazole-based small molecule HTMs possessing a deep HOMO level, which were *N*,*N*′-dicarbazolyl-3,5-benzene (mCP), 4,4′-*N*,*N*′-dicarbazole-biphenyl (CBP), and TCTA. Their HOMO energy values measured by an AC-2 photoelectron spectrometer are −5.93, −5.97, and −5.70, respectively, which are sufficiently low to inject holes into QDs. For the feasibility study of the QD-transplanting onto the vacuum-deposited HTLs, we transplanted green QDs onto each HTL using the PDMS stamp which has line-and-space patterns with widths of 6, 4, and 2 μm. The wettability and patternability of the QDs onto each HTL were observed with a fluorescent optical microscope (FOM). The FOM images in Figure 2 clearly show the difference between the patterns of the transplanted QDs. On the mCP layer, the QD stripes are nonuniformly and sparsely patterned, and thus they show weak fluorescence (Figure 2a). For the case using CBP, the QD patterns are more uniform than those on the mCP film, but the edges of the patterns are quite rough and partly broken especially in the narrow stripes (Figure 2b). On the other hand, when we use TCTA as the HTL, the QD stripes are highly uniform and their edges are fine for all widths of the patterns without any noticeable defects (Figure 2c). Insets in each figure show the magnified FOM images of the 4 μm stripes. After transplanting the QDs to each HTL, the PDMS stamps were also examined with the FOM to ascertain the existence of residual (i.e, untransferred) QDs. As expected, a lot of QDs remained on the PDMS stamp imprinted on the mCP layer, while few QDs existed on the stamp used for the TCTA film (see Figure S2).

In order to determine the reason for these drastic differences depending on the receiving organic layer, we measured the contact angles and calculated the work of adhesion values with the following equation[32]

$$W_{1,2} = 4\left(\frac{\gamma_1^d\gamma_2^d}{\gamma_1^d + \gamma_2^d} + \frac{\gamma_1^p\gamma_2^p}{\gamma_1^p + \gamma_2^p}\right) \quad (1)$$

where $W_{1,2}$ is the work of adhesion between materials 1 and 2, γ is the surface energy with the superscripts of d and p for the dispersion and polar components, respectively. The contact angles on various films (mCP, CBP, TCTA, and QDs on PDMS) were obtained by using the low-bond axisymmetric drop shape analysis (LBADSA) method[33] which is based on the fitting of the Young−Laplace equation to the droplet images with polar and nonpolar probing liquids (deionized (DI) water and ethylene glycol (EG), respectively). The calculated work of adhesion values between each HTM and the QDs on PDMS, i.e., $W_{mCP,QD}$, $W_{CBP,QD}$, and $W_{TCTA,QD}$, were 10.7, 11.2, and 11.4 mJ m^{-2}, respectively, as compared in Figure 2d. From the result, we can know that the mCP film has weaker adhesion with the QDs compared to the other organic films, and therefore, the QDs were poorly transferred onto the mCP layer. Meanwhile, the $W_{TCTA,QD}$ is slightly higher than the $W_{CBP,QD}$, which resulted in the fine patterns of QDs on TCTA as shown in the FOM images. The contact angles with dispersive and polar solvents, surface energy, and work of adhesion values are summarized in Table 1. We also examined the patternability of red- and blue-emitting QDs onto the TCTA film in the same method, and found that these QDs also formed fine and clear patterns on TCTA as shown in Figure 2e,f.

Table 1. Contact Angles, Surface Energies, And Works of Adhesion Values of the HTMs and the QDs on a PDMS Stamp

	contact angle [deg]				
HTL	DI water	EG	γ^d (dispersion component) [mJ m^{-2}]	γ^p (polar component) [mJ m^{-2}]	work of adhesion[a] [mJ m^{-2}]
mCP	87.9	65.0	4.91	1.32	10.7
CBP	89.1	61.7	6.60	0.72	11.2
TCTA	90.7	58.9	8.47	0.28	11.4
QDs on PDMS	97.0	77.3	3.82	0.84	-

[a]Work of adhesion between each HTL and the QDs on a PDMS stamp.

Although the transplanted QD patterns on mCP and CBP are quite rough and inhomogeneous, we fabricated and characterized the green QLED devices with all HTLs for comparison. To fabricate the QLED devices, 1,3,5-tris(*N*-phenylbenzimidazol-2yl) benzene (TPBi) as an electron transport layer, LiF as an electron injection layer, and Al cathodes were deposited sequentially on top of the QD layer. A schematic device structure and the device performance are shown in Figure 3. Because the QDs were hardly transplanted on the mCP layer, the current density of the device with mCP is much larger than that of the other devices (Figure 3b), whereas its luminance and efficiency are very poor (Figure S3). Besides, we could not observe any emission from the green QDs except for the blue peak originating from the adjacent organic layers (Figure 3c). In the case of the CBP layer on which the QDs were partly transplanted, the device emitted a green color mainly from the QDs and a weak blue color from

DOI: 10.1021/acsami.5b01738
ACS Appl. Mater. Interfaces 2015, 7, 10828−10833

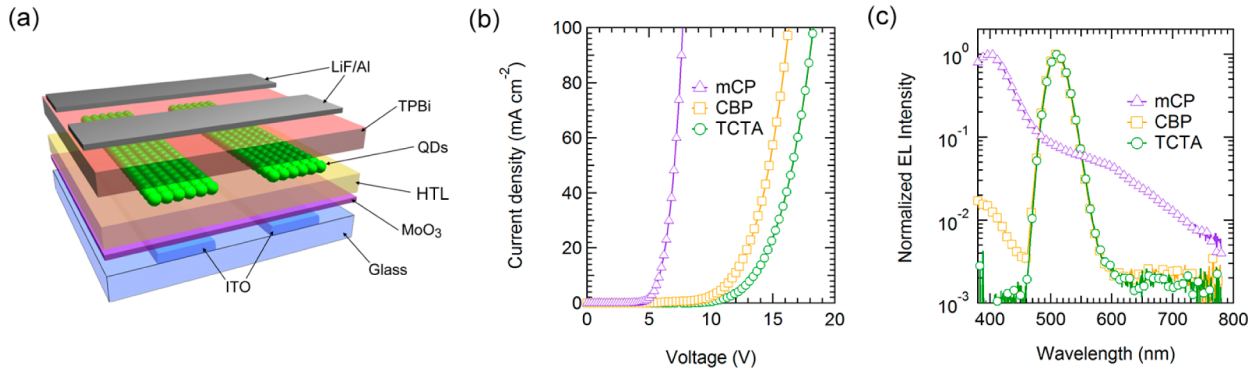

Figure 3. (a) Scheme of the QLED device structure, and the characteristics of the green QLEDs with mCP, CBP, and TCTA as the HTL in terms of the (b) current density–voltage and (c) normalized EL spectra in log-scale measured at 5 mA cm^{-2}.

the adjacent organic layers, which are attributed to the imperfect QD-deposition on the CBP layer. The QLED with the TCTA layer, as verified already, exhibits better performance compared to the other HTMs-based devices. Additionally, in terms of material stability, TCTA has a higher glass transition temperature (T_g) of 151 °C than CBP (62 °C) and mCP (60 °C).[34,35] Because the vacuum-deposited HTLs should be exposed to the ambient condition during the QD printing process (even though it is conducted in the glovebox filled with inert gas), the device performance is significantly affected by thermal stability of organic materials which are likely to be crystallized and degraded in the ambient condition (see Figure S4). Thus, higher efficiency can be obtained in the QLEDs with TCTA possessing high T_g as the HTL.

Based on the results, we fabricated the R, G, and B QLEDs in the same device structure by transplanting each QD layer onto TCTA. Figure 4 shows the device performance in terms of the current density–voltage, luminance–voltage, luminous efficiency (LE)–current density, and normalized electroluminescence (EL) spectra. The current density at a certain applied voltage is high in the sequence of the red, green, and blue devices, because the hole injection barrier from the HOMO level of the HTL to the valence band (VB) level of each QD is different due to the difference in the intrinsic band gap of the QDs. From the luminance–voltage characteristics, we obtained the maximum luminance of 2497, 14102, and 265 cd m^{-2} for the R, G, and B QLEDs, respectively. The maximum LE values of the transplanted R, G, and B QLEDs are 1.83, 8.07, and 0.19 cd A^{-1} as plotted in Figure 4c, which correspond to 1.93%, 2.33%, and 0.32% in terms of the external quantum efficiency (EQE), respectively. The performance of the transplanted devices is not as high as that of the recent reports without patterning the QD layer,[5,9] but the performance of our QLEDs is comparable to or even better than the patterned QLEDs in terms of the efficiency and brightness.[18−30] As shown in Figure 4d, all devices exhibit deeply saturated colors by the narrow EL emission profile with the Gaussian full-width-at-half-maximum (fwhm) bandwidths of about 30 nm. Most of the emission originated from the QD layers owing to the good patterning property of the QDs onto TCTA, which offers the possibility to fabricate full-color display devices with wide color gamut. The peak emission wavelengths are 637, 519, and 436 nm for R, G, and B QLEDs, respectively. The corresponding Commission Internationale de l'Eclairage (CIE) coordinates are (0.68, 0.31), (0.15, 0.72), and (0.19, 0.06) for R, G, and B devices, which mostly cover the color gamut of the National Television Standards Committee (NTSC) 1953 standard color space (Figure S4). The device performance of the transplanted R, G, and B QLEDs is also summarized in Table S1.

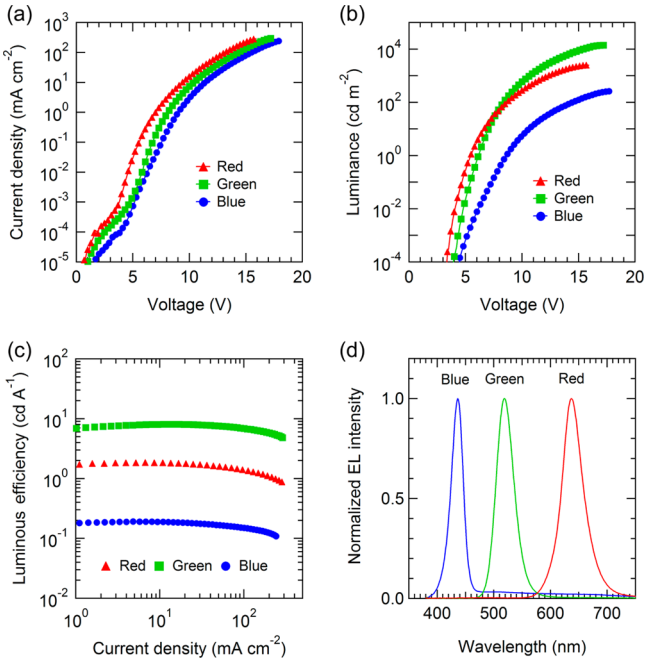

Figure 4. Optical and electrical characteristics of the R, G, and B QLEDs on the TCTA HTL fabricated by the transplanting method: (a) current density–voltage, (b) luminance–voltage, (c) luminous efficiency–current density, and (d) normalized EL spectra measured at the current density of 50 mA cm^{-2}.

CONCLUSION

We introduced a soft contact QD-transplanting technique onto the vacuum-deposited small molecules without pressure and demonstrated the full-color QLEDs using this method. We also studied the patternability of the QDs on the mCP, CBP, and TCTA layers by investigating their surface properties. Among the HTMs, TCTA showed the best QD-patternability and QLED performance due to the high work of adhesion and high T_g. In addition, the QD-transplanting on TCTA served the uniform and homogeneous QD patterns down to a few micrometers for all the RGB QDs. Based on the results, the R, G, and B QLEDs were successfully fabricated by transplanting each QD onto the soft TCTA layer, exhibiting higher brightness and efficiency than those of the previous QLEDs

DOI: 10.1021/acsami.5b01738
ACS Appl. Mater. Interfaces 2015, 7, 10828−10833

fabricated by other patterning methods. We believe that the transplanting technique with the fundamental studies and engineering presented here is meaningful for the realization of the colloidal QD-based full-color displays and other optoelectronic devices.

EXPERIMENTAL SECTION

Preparation of Red, Green, and Blue QDs. Red, green, and blue-emitting QDs were synthesized in the structures of CdSe/CdS/ZnS, CdSe@ZnS, and $Cd_{1-x}Zn_xS$@ZnS, respectively, by using or slightly modifying the previously reported methods.[6,7] Their sizes were 8 nm for red and blue QD, and 9 nm for green QD.

QD-Transplanting. A Si/SiO_2 substrate was treated with UV-ozone for 10 min and rinsed with DI water. The cleaned substrate was immersed in a 2 mM solution of OTS in hexadecane for 2 h to make the surface hydrophobic, followed by the sonication in chloroform, isopropyl alcohol, and methanol for 10 min each and drying at 120 °C. The QD dispersion in hexane (10 mg mL^{-1}) was spin-coated onto the OTS-SAM treated SiO_2 substrate at a rate of 4000 rpm for 30 s. For the PDMS stamp, Sylgard 184 A and B were mixed with a volume ratio of 10:1, and then they were poured onto a Si master substrate patterned by photolithography and cured at 60 °C for 1 h. For better adhesion between the PDMS stamp and QDs, the surface of the PDMS was treated with UV-ozone for 4 min.

Fabrication and Characterization of QLEDs. By the thermal vacuum evaporation, the MoO_3 (10 nm) and TCTA (40 nm) were deposited in sequence on a patterned ITO-glass substrate under the pressure of 3×10^{-6} Torr. The QD layer was then deposited on the ITO/MoO_3/TCTA layers by the transplanting method, followed by the thermal evaporation of TPBi (40 nm), LiF (0.5 nm), and Al (100 nm) successively at a rate of 1, 0.05, and 3 Å/s, respectively. The current−voltage−luminance characteristics were measured with a Keithley 236 source-measure unit and a Keithley 2000 multimeter coupled with a calibrated Si photodiode. The EL spectra of the devices were obtained using a Konica-Minolta CS-1000A spectroradiometer.

ASSOCIATED CONTENT

Supporting Information

AFM images, FOM images of residual QDs on PDMS stamps, the characteristics of the green QLEDs with different HTLs, CIE color coordinates of QLEDs, the air stability of HTMs, and the summary of device performance of QLEDs. The Supporting Information is available free of charge on the ACS Publications website at DOI: 10.1021/acsami.5b01738.

AUTHOR INFORMATION

Corresponding Authors

*E-mail: jkwak@dau.ac.kr.
*E-mail: chlee7@snu.ac.kr.

Author Contributions

¶H. Cho and J. Kwak contributed equally to this work.

Notes

The authors declare no competing financial interest.

ACKNOWLEDGMENTS

This work was supported by the Industrial Strategic Technology Development Program (10045145) funded by the Ministry of Trade, Industry and Energy (MOTIE, Korea), and by the Basic Science Research Program through the National Research Foundation of Korea (NRF-2011-0022716) funded by the Ministry of Education. This work was also supported in part by the NRF funded by the Korea Ministry of Science, ICT & Future through the Technology Development Program to Solve Climate Changes (NRF-2009-C1AAA001-2009-0093282).

REFERENCES

(1) Coe, S.; Woo, W.-K.; Bawendi, M. G.; Bulović, V. Electroluminescence from Single Monolayers of Nanocrystals in Molecular Organic Devices. *Nature* **2002**, *420*, 800−803.
(2) Sun, Q.; Wang, Y. A.; Li, L. S.; Wang, D.; Zhu, T.; Xu, J.; Yang, C.; Li, Y. Bright, Multicoloured Light-Emitting Diodes Based on Quantum Dots. *Nat. Photonics* **2007**, *1*, 717−722.
(3) Mashford, B. S.; Stevenson, M.; Popovic, Z.; Hamilton, C.; Zhou, Z.; Breen, C.; Steckel, J.; Bulovic, V.; Bawendi, M.; Coe-Sullivan, S.; Kazlas, P. T. High-Efficiency Quantum-Dot Light-Emitting Devices with Enhanced Charge Injection. *Nat. Photonics* **2013**, *7*, 407−412.
(4) Kim, S.; Im, S. H.; Kim, S.-W. Performance of Light-Emitting-Diode Based on Quantum Dots. *Nanoscale* **2013**, *5*, 5205−5214.
(5) Dai, X.; Zhang, Z.; Jin, Y.; Niu, Y.; Cao, H.; Liang, X.; Chen, L.; Wang, J.; Peng, X. Solution-Processed, High-Performance Light-Emitting Diodes Based on Quantum Dots. *Nature* **2014**, *515*, 96−99.
(6) Bae, W. K.; Char, K.; Hur, H.; Lee, S. Single-Step Synthesis of Quantum Dots with Chemical Composition Gradients. *Chem. Mater.* **2008**, *20*, 531−539.
(7) Bae, W. K.; Nam, M. K.; Char, K.; Lee, S. Gram-Scale One-Pot Synthesis of Highly Luminescent Blue Emitting $Cd_{1-x}Zn_xS$/ZnS Nanocrystals. *Chem. Mater.* **2008**, *20*, 5307−5313.
(8) Lim, J.; Jun, S.; Jang, E.; Baik, H.; Kim, H.; Cho, J. Preparation of Highly Luminescent Nanocrystals and Their Application to Light-Emitting Diodes. *Adv. Mater.* **2007**, *19*, 1927−1932.
(9) Lee, K.-H.; Lee, J.-H.; Song, W.-S.; Ko, H.; Lee, C.; Lee, J.-H.; Yang, H. Highly Efficient, Color-Pure, Color-Stable Blue Quantum Dot Light-Emitting Devices. *ACS Nano* **2013**, *7*, 7295−7302.
(10) Lee, K.-H.; Lee, J.-H.; Kang, H.-D.; Park, B.; Kwon, Y.; Ko, H.; Lee, C.; Lee, J.; Yang, H. Over 40 cd/A Efficient Green Quantum Dot Electroluminescent Device Comprising Uniquely Large-Sized Quantum Dots. *ACS Nano* **2014**, *8*, 4893−4901.
(11) Kwak, J.; Bae, W. K.; Zorn, M.; Woo, H.; Yoon, H.; Lim, J.; Kang, S. W.; Weber, S.; Butt, H.-J.; Zentel, R.; Lee, S.; Char, K.; Lee, C. Characterization of Quantum Dot/Conducting Polymer Hybrid Films and Their Application to Light-Emitting Diodes. *Adv. Mater.* **2009**, *21*, 5022−5026.
(12) Bae, W. K.; Kwak, J.; Lim, J.; Lee, D.; Nam, M. K.; Char, K.; Lee, C.; Lee, S. Multicolored Light-Emitting Diodes Based on All-Quantum-Dot Multilayer Films Using Layer-by-Layer Assembly Method. *Nano Lett.* **2010**, *10*, 2368−2373.
(13) Bae, W. K.; Lim, J.; Zorn, M.; Kwak, J.; Park, Y.-S.; Lee, D.; Lee, S.; Char, K.; Zentel, R.; Lee, C. Reduced Efficiency Roll-Off in Light-Emitting Diodes Enabled by Quantum Dot-Conducting Polymer Nanohybrids. *J. Mater. Chem. C* **2014**, *2*, 4974−4979.
(14) Bae, W. K.; Park, Y.-S.; Lim, J.; Lee, D.; Padilha, L. A.; McDaniel, H.; Robel, I.; Lee, C.; Pietryga, J. M.; Klimov, V. I. Controlling The Influence of Auger Recombination on the Performance of Quantum-Dot Light-Emitting Diodes. *Nat. Commun.* **2013**, *4*, 2661.
(15) Bae, W. K.; Kwak, J.; Park, J. W.; Char, K.; Lee, C.; Lee, S. Highly Efficient Green-Light-Emitting Diodes Based on CdSe@ZnS Quantum Dots with a Chemical-Composition Gradient. *Adv. Mater.* **2009**, *21*, 1690−1694.
(16) Qian, L.; Zheng, Y.; Xue, J.; Holloway, P. H. Stable and Efficient Quantum-Dot Light-Emitting Diodes Based on Solution-Processed Multilayer Structures. *Nat. Photonics* **2011**, *5*, 543−548.
(17) Kwak, J.; Bae, W. K.; Lee, D.; Park, I.; Lim, J.; Park, M.; Cho, H.; Woo, H.; Yoon, D. Y.; Char, K.; Lee, S.; Lee, C. Bright and Efficient Full-Color Colloidal Quantum Dot Light-Emitting Diodes Using an Inverted Device Structure. *Nano Lett.* **2012**, *12*, 2362−2366.
(18) Kim, T.-H.; Cho, K.-S.; Lee, E. K.; Lee, S. J.; Chae, J.; Kim, J. W.; Kim, D. H.; Kwon, J.-Y.; Amaratunga, G.; Lee, S. Y.; Choi, B. L.; Kuk, Y.; Kim, J. M.; Kim, K. Full-Colour Quantum Dot Displays Fabricated by Transfer Printing. *Nat. Photonics* **2011**, *5*, 176−182.
(19) Haverinen, H. M.; Myllylä, R. A.; Jabbour, G. E. Inkjet Printing of Light Emitting Quantum Dots. *Appl. Phys. Lett.* **2009**, *94*, 073108.
(20) Wood, V.; Panzer, M. J.; Chen, J.; Bradley, M. S.; Halpert, J. E.; Bawendi, M. G.; Bulović, V. Inkjet-Printed Quantum Dot−Polymer

DOI: 10.1021/acsami.5b01738
ACS Appl. Mater. Interfaces 2015, 7, 10828−10833

Composites for Full-Color AC-Driven Displays. *Adv. Mater.* **2009**, *21*, 2151−2155.
(21) Haverinen, H. M.; Myllylä, R. A.; Jabbour, G. E. Inkjet Printed RGB Quantum Dot-Hybrid LED. *J. Disp. Technol.* **2010**, *6*, 87−89.
(22) Kim, T.-H.; Chung, D.-Y.; Ku, J.; Song, I.; Sul, S.; Kim, D.-H.; Cho, K.-S.; Choi, B. L.; Min Kim, J.; Hwang, S.; Kim, K. Heterogeneous Stacking of Nanodot Monolayers by Dry Pick-and-Place Transfer and Its Applications in Quantum Dot Light-Emitting Diodes. *Nat. Commun.* **2013**, *4*, 2637.
(23) Lee, S.; Yoon, D.; Choi, D.; Kim, T.-H. Mechanical Characterizations of High-Quality Quantum Dot Arrays via Transfer Printing. *Nanotechnology* **2013**, *24*, 025702.
(24) Anikeeva, P. O.; Madigan, C. F.; Halpert, J. E.; Bawendi, M. G.; Bulović, V. Electronic and Excitonic Processes in Light-Emitting Devices Based on Organic Materials and Colloidal Quantum Dots. *Phys. Rev. B* **2008**, *78*, 085434.
(25) Kim, L.; Anikeeva, P. O.; Coe-Sullivan, S. A.; Steckel, J. S.; Bawendi, M. G.; Bulović, V. Contact Printing of Quantum Dot Light-Emitting Devices. *Nano Lett.* **2008**, *8*, 4513−4517.
(26) Panzer, M. J.; Aidala, K. E.; Bulović, V. Contact Printing of Colloidal Nanocrystal Thin Films for Hybrid Organic/Quantum Dot Optoelectronic Devices. *Nano Rev.* **2012**, *3*, 16144.
(27) Rizzo, A.; Mazzeo, M.; Biasiucci, M.; Cingolani, R.; Gigli, G. White Electroluminescence from a Microcontact-Printing-Deposited CdSe/ZnS Colloidal Quantum-Dot Monolayer. *Small* **2008**, *4*, 2143−2147.
(28) Rizzo, A.; Mazzeo, M.; Palumbo, M.; Lerario, G.; D'Amone, S.; Cingolani, R.; Gigli, G. Hybrid Light-Emitting Diodes from Microcontact-Printing Double-Transfer of Colloidal Semiconductor CdSe/ZnS Quantum Dots onto Organic Layers. *Adv. Mater.* **2008**, *20*, 1886−1891.
(29) Steckel, J. S.; Snee, P.; Coe-Sullivan, S.; Zimmer, J. P.; Halpert, J. E.; Anikeeva, P.; Kim, L.-A.; Bulovic, V.; Bawendi, M. G. Color-Saturated Green-Emitting QD-LEDs. *Angew. Chem., Int. Ed.* **2006**, *45*, 5796−5799.
(30) Kong, Y. L.; Tamargo, I. A.; Kim, H.; Johnson, B. N.; Gupta, M. K.; Koh, T.-W.; Chin, H.-A.; Steingart, D. A.; Rand, B. P.; McAlpine, M. C. 3D Printed Quantum Dot Light-Emitting Diodes. *Nano Lett.* **2014**, *14*, 7017−7023.
(31) Lee, M. J.; Kim, J.; Lee, J. S.; Kim, Y. S. Pressure-Assisted Printing with Crack-Free Metal Electrodes Using an Anti-Adhesive Rigiflex Stamp. *J. Mater. Chem.* **2010**, *20*, 2746−2748.
(32) Wu, S. Polar and Nonpolar Interactions in Adhesion. *J. Adhes.* **1973**, *5*, 39−55.
(33) Stalder, A. F.; Melchior, T.; Müller, M.; Sage, D.; Blu, T.; Unser, M. Low-Bond Axisymmetric Drop Shape Analysis for Surface Tension and Contact Angle Measurements of Sessile Drops. *Colloids Surf., A* **2010**, *364*, 72−81.
(34) Kuwabara, Y.; Ogawa, H.; Inada, H.; Noma, N.; Shirota, Y. Thermally Stable Multilared Organic Electroluminescent Devices Using Novel Starburst Molecules, 4,4′,4″-Tri(N-Carbazolyl)-Triphenylamine (TCTA) and 4,4′,4″-Tris(3-Methylphenylphenylamino)Triphenyl Amine (M-MTDATA), as Hole-Transport Materials. *Adv. Mater.* **1994**, *6*, 677−679.
(35) Tsai, M.-H.; Hong, Y.-H.; Chang, C.-H.; Su, H.-C.; Wu, C.-C.; Matoliukstyte, A.; Simokaitiene, J.; Grigalevicius, S.; Grazulevicius, J. V.; Hsu, C.-P. 3-(9-Carbazolyl)Carbazoles and 3,6-Di(9-Carbazolyl)-Carbazoles as Effective Host Materials for Efficient Blue Organic Electrophosphorescence. *Adv. Mater.* **2007**, *19*, 862−866.

DOI: 10.1021/acsami.5b01738
ACS Appl. Mater. Interfaces 2015, 7, 10828−10833